LIMNOLOGY and OCEANOGRAPHY

ASLO

Limnol. Oceanogr. 71, 2026, e70297

doi: 10.1002/lno.70297

RESEARCH ARTICLE

Marginal seas as potential sinks for refractory carbon

Yeongjin Ryu,[1] **Heejun Han**,[2] **Taehee Na**,[1] **Guebuem Kim**,[1] **Jeomshik Hwang**[1*]

[1]School of Earth and Environmental Sciences/Research Institute of Oceanography, Seoul National University, Seoul, Republic of Korea; [2]Marine Environmental Research Department, Korea Institute of Ocean Science and Technology (KIOST), Busan, Republic of Korea

Abstract

The Yellow Sea (YS) and East China Sea (ECS) are marginal seas in the Northwestern Pacific that receive large amounts of aged, terrestrial organic matter. In this study, we measured dissolved organic carbon (DOC) concentrations and radiocarbon contents ($\Delta^{14}C$) in these seas during summer and autumn, extending a previous winter study to provide a more comprehensive understanding of the DOC cycle, including its sources and removal. The significant negative correlation between DOC concentrations or $\Delta^{14}C$ values and salinity shows that vertical and horizontal water mass mixing between coastal waters and the water intruding to the site from the Northwestern Pacific is the primary control on the distribution of DOC. The $\Delta^{14}C$ values and the inverse of DOC concentrations show significant negative correlation, suggesting that marine primary production is the dominant DOC source in this region. However, deviations from this correlation imply inputs of aged DOC. Although freshwater input is highest in summer, the effects of aged DOC are greater in autumn and winter. Terrestrial organic matter delivered by rivers is rapidly degraded, and this process likely stimulates marine primary production. In addition, large seasonal differences in $\Delta^{14}C$ values in Kuroshio-derived waters indicate significant removal of marine refractory DOC on the continental shelf. The results show that continental shelves have a key role in the removal of terrestrial and marine refractory DOC.

Dissolved organic carbon (DOC) in the ocean is the largest reduced carbon reservoir in the marine environment (Hansell et al. 2009). In waters below 1500 m depth, DOC concentration decreases along the deep oceanic circulation pathway from the North Atlantic to the North Pacific (Hansell and Carlson 1998). The radiocarbon (^{14}C) age of DOC increases from 4900 to 6400 yr BP (BP means before present, i.e., 1950), indicative of progressive aging (Bauer et al. 1992; Druffel et al. 1992, 2016; Williams and Druffel 1987). Based on the similarities in the vertical profiles of DOC concentration and radiocarbon ($\Delta^{14}C$; per mil [‰] deviation from the 1950 atmospheric CO_2 standard; Stuiver and Polach 1977), as well as the $\Delta^{14}C$ values of dissolved inorganic carbon (DIC) and stable carbon isotope ratios ($\delta^{13}C$), it is inferred that most oceanic DOC is derived from primary production in surface waters and undergoes multiple cycles of deep oceanic circulation (Bauer et al. 1992; Druffel et al. 1992; Williams and Druffel 1987).

In coastal environments, terrestrial DOC from rivers, atmospheric deposition, and groundwater may be important sources of DOC, in addition to the DOC produced within the ocean (Hedges and Keil 1995; Kwon et al. 2021; Lønborg et al. 2020). The annual flux of riverine DOC is estimated to be 0.22–0.40 Pg C (Bauer and Bianchi 2011; Bauer et al. 2013; Liu et al. 2024; Meybeck 1982), while atmospheric and groundwater contributions are estimated to be approximately 0.1 Pg C yr^{-1} (Chen et al. 2018; Willey et al. 2000). These allochthonous DOC influx to the ocean is smaller than the global export rate of semi-labile DOC into the interior ocean below 100 m (~ 1.8 Pg C yr^{-1}; Hansell et al. 2009) and higher than the steady state input of marine DOC pool (i.e., DOC reservoir divided by its ^{14}C age; ~ 0.1 Pg C yr^{-1}; Williams and Druffel 1987). However, after entering the ocean, terrestrial DOC is known to be rapidly degraded on decadal timescales by marine microbes or photochemical processes (Bianchi 2011). The degradation of terrestrial DOC can release nutrients, stimulating marine production. Also, enhanced primary production subsequently facilitates the priming effect in which the presence of labile substrates

*Correspondence: jeomshik@snu.ac.kr

Associate editor: Michael Seidel

promotes the degradation of more recalcitrant DOC (Bauer and Bianchi 2011; Bianchi 2011; Shen and Benner 2018). The study of lignin phenols in the open ocean suggested that a small fraction (0.7% to 2.4%) of terrestrial DOC persists even in the deep ocean (Opsahl and Benner 1997).

At a global context, terrestrial DOC is a minor contributor. However, its contribution may vary significantly in the coastal ocean where water residence time is short compared to the open ocean, and direct input of terrestrial DOC is persistent. Radiocarbon-based studies have provided important insights into DOC cycling on continental shelves, including its sources and residence time in the ocean (Bauer et al. 2002; Guo et al. 1996; McNichol and Aluwihare 2007). For example, a study in the Mid-Atlantic Bight examined the seasonal variations and vertical distributions of $\Delta^{14}C$ and $\delta^{13}C$ values of DOC, DIC, and particulate organic carbon (POC), and assessed the contributions of various organic carbon sources (Bauer et al. 2002). Their results showed that $\Delta^{14}C$ values of DOC increased toward the coast, with the highest $\Delta^{14}C$ values observed in low-salinity shelf waters, suggesting that fresh DOC input from rivers during spring and summer led to an increase in $\Delta^{14}C$ values. Similarly, Guo et al. (1996) analyzed $\delta^{13}C$, $\Delta^{14}C$, and C : N values of colloidal organic matter with the size between 1 kDa and 0.2 μm in the Mid-Atlantic Bight, and identified a decreasing trend of $\Delta^{14}C$ values with decreasing colloid size and from estuarine to offshore waters. A recent study combined radiocarbon analysis and molecular characterization of solid-phase extracted DOM in the Northeastern Atlantic shelves (Wei et al. 2024). This study demonstrated fresh DOM intrusion to the deep ocean along the down-slope transport, highlighting an additional mechanism of continental-shelf borne DOM transport.

The Yellow Sea (YS) and East China Sea (ECS) are among the largest continental shelves in the world located between China and the Korean Peninsula. This region mediates export of terrestrial organic matter to the Northwestern Pacific. A few studies have examined the $\Delta^{14}C$ values of terrestrial DOC sources in this region, showing that allochthonous DOC originating from regions in China is introduced primarily through the Yangtze River (Changjiang River) and Yellow River, with $\Delta^{14}C$ values ranging from −183‰ to −44‰ and −195‰ to −158‰, respectively (Wang et al. 2012, 2016a; Xue et al. 2017). These low $\Delta^{14}C$ values contrast with the modern DOC that results from marine primary production (Butman et al. 2015; Williams and Druffel 1987; Xue et al. 2017). Surface sediments in the YS and ECS contain aged, land-derived organic matter with low $\Delta^{14}C$ values (−305‰ ± 102‰) (Bao et al. 2016). However, porewater DOC in surface sediments (0–2 cm) has higher $\Delta^{14}C$ values (−66‰ to −12‰), indicating the transformation of younger POC into DOC (Fu et al. 2022).

Besides these studies that reported $\Delta^{14}C$ values of DOC sources in the YS and ECS, ^{14}C-based investigations of DOC cycling in this region remain limited. Han et al. (2022) measured the distributions of Ra isotopes, DOC concentrations, carbon isotopic ratios ($\delta^{13}C$ and $\Delta^{14}C$), and fluorescent dissolved organic matter (FDOM) in the southern YS and ECS in winter 2017. Their study suggested that the $\Delta^{14}C$ distribution of DOC in the ECS is regulated by water mass mixing between Yellow Sea Water and Kuroshio Current Water. Using a measured $\Delta^{14}C$ value of −271‰ ± 18‰ for DOC in Kuroshio Current Water, they estimated the $\Delta^{14}C$ value of DOC in Yellow Sea Water to be −170‰ ± 50‰. Based on the end-member mixing approach, about 1.9 ± 0.8 Tg C of DOC was suggested to be exported from the Yellow Sea to the East China Sea per year (Han et al. 2022).

In this study, we measured the DOC concentrations and $\Delta^{14}C$ values in the central YS and ECS in August 2020 and November 2021. By integrating these results with previously reported DOC data from the southern YS and ECS in February 2017 (Han et al. 2022), we examined the processes regulating DOC cycling on the continental shelf of the Northwestern Pacific, which is strongly affected by the input of terrestrial organic matter. We discuss the distribution of DOC concentrations and $\Delta^{14}C$ values with respect to salinity, and the relationships between DOC concentrations and $\Delta^{14}C$ values in the form of the Keeling plot (Keeling 1958; Mortazavi and Chanton 2004). This approach allows us to describe seasonal variation, evaluate the contribution of various DOC sources, and further assess potential removal processes of marine refractory DOC.

Methods

Sample collection and analysis

Measurements of oceanographic parameters and seawater sampling were conducted aboard RV *Onnuri* during August 13–18, 2020 and November 25–27, 2021 in the YS and ECS (the line connecting the Changjiang Estuary and Jeju Island marks the boundary between the YS and ECS; Fig. 1). The YS has an average depth of 44 m and a surface area of 3.8×10^5 km^2, while the ECS covers an area of 7.7×10^5 km^2 (Chen 2009; Lie and Cho 2016). At Sta. #21 (152 m depth), samples were collected at four depths. At stations #1-1 (47 m depth) and #5-3 (44 m depth), located near the Korean Peninsula in the YS, samples were collected from both the ocean surface and bottom (~ 3 m above the seafloor). At the remaining stations, samples were collected from three depths: the surface, ~ 50 m depth, and ~ 3 m above the seafloor.

Seawater samples for DOC ^{14}C measurements were filtered through GF/F filters (142 mm, 0.7 μm pore size; Whatman) from Niskin bottles and stored in 1-L Boston Round bottles (Wheaton) at − 20°C until analysis (Druffel et al. 2019; Ryu et al. 2023). For DOC concentration measurements, seawater samples filtered through GF/F filters were collected into 20-mL glass ampules (Fisher Scientific). To suppress microbial activity, 20 μL of 6 N HCl (HPLC grade; Sigma-Aldrich) was added, and the ampules were flame-sealed and stored at room temperature in the dark until analysis (Halewood et al. 2022; Han et al. 2022). Sampling bottles, ampules, and filters were all pre-combusted at 450°C for 4 h before use.

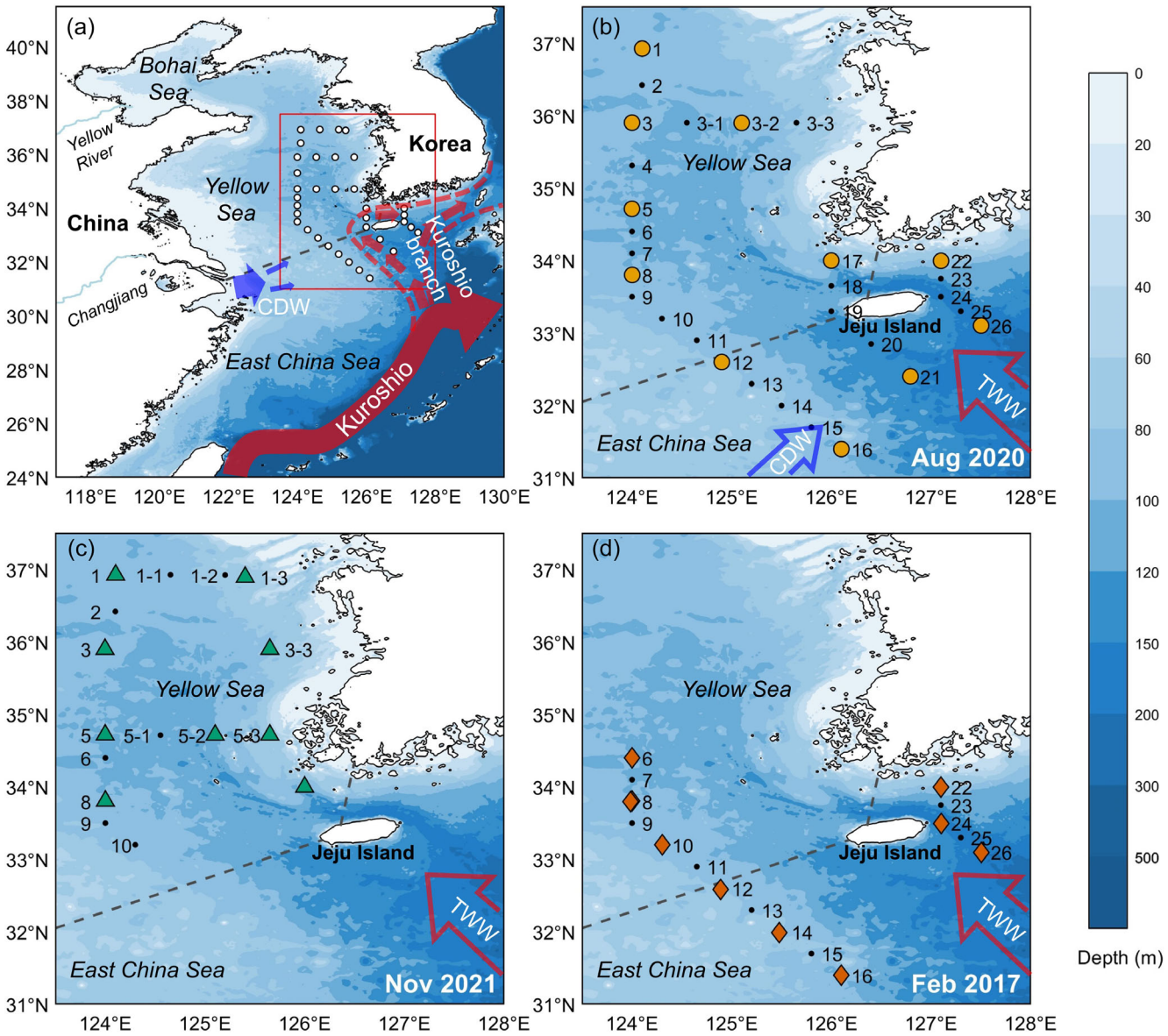

Fig. 1. (**a**) Map of the study region in the Northwestern Pacific. The red rectangle indicates the area shown in (**b**) to (**d**). Kuroshio current and its branch, Tsushima Warm Water (TWW), and Changjiang Diluted Water (CDW) are indicated by thick arrows. Sampling stations are shown for cruises undertaken in (**b**) August 2020, (**c**) November 2021, and (**d**) February 2017 (data are from Han et al. 2022). Seawater samples for radiocarbon analysis were collected at the sites indicated by the large symbols. The black dots indicate stations where only hydrographic measurements were conducted. The dashed line indicates the boundary between the East China Sea and Yellow Sea. The original name, location, and bottom depth of each station are given in the Supporting Information.

For radiocarbon analysis, DOC in seawater was converted to CO_2 using the ultraviolet oxidation method (Beaupré et al. 2007; Ryu et al. 2023). Seawater samples were thawed immediately before analysis, and 600–800 mL of the sample was transferred to a quartz reactor. Subsequently, 85% phosphoric acid (HPLC grade; Sigma Aldrich) was added to lower the pH to < 2. Nitrogen gas (99.999% purity) was then bubbled through the sample at 400 mL min^{-1} for 90 min to remove DIC, and the samples were irradiated with ultraviolet light (1200 W; mercury arc lamp; Lichtzen) for 6 h. The oxidized CO_2 was extracted by bubbling nitrogen gas at 120 mL min^{-1} for 120 min, and was then cryogenically purified and quantified manometrically before being stored in a Pyrex tube. The recovery of DOC in the samples was estimated to be 100% ± 8% ($n = 48$) as compared with the concentration measured using the high-temperature catalytic oxidation method. Radiocarbon analysis was conducted at the National Ocean Sciences Accelerator Mass Spectrometry (NOSAMS)

Facility at the Woods Hole Oceanographic Institution, Woods Hole, USA, and the Keck Carbon Cycle Accelerator Mass Spectrometer facility at the University of California, Irvine, USA.

Radiocarbon ratios were reported in $\Delta^{14}C$ notation following Stuiver and Polach (1977). Fraction modern (*Fm*) was measured relative to the oxalic acid standard, and $\Delta^{14}C$ values were calculated using:

$$\Delta^{14}C = \left(Fm\, e^{(1950-y)/8267} - 1\right) \times 1000 \quad (1)$$

where y is the year of measurement. Conventional radiocarbon age, representing the apparent age relative to 1950, was calculated using:

$$^{14}C\,\text{age}\,(\text{yr BP}) = -8033\,\ln(Fm) \quad (2)$$

The blank analysis was calibrated using D-(+)-glucose (≥ 99.5%; CAS# 50-99-7; GC grade; Sigma Aldrich) and glycine (> 99%; Lot# A0302450; Acros Organics) as standards (Hwang and Druffel 2005; Ryu et al. 2023). Approximately one glucose and one glycine standard were analyzed for every eight samples using the same method. The blank correction was applied by comparing the results with those obtained directly from combustion of a large amount of standards (~ 1 mg C). The estimated blank was 6.6 ± 0.8 μg C with a $\Delta^{14}C$ value of −657‰ ± 45‰, which is less than 2% of the size of DOC extracted (360–800 μg). The change in the $\Delta^{14}C$ values of the samples after blank correction was < 8‰. The difference between duplicate samples (i.e., two pairs analyzed at NOSAMS and two pairs at UC Irvine) was 1‰, 3‰, 8‰, and 8‰, respectively.

The DOC concentrations were measured using the high-temperature catalytic oxidation method with a TOC analyzer (TOC-L; Shimadzu) (Han et al. 2022). The precision of the instrument was determined by repeatedly measuring the deep-sea reference seawater standard supplied by the University of Miami (41–44 μM), which yielded results within 2% of the average DOC concentration.

Keeling plot approach

The vertical distribution of DOC $\Delta^{14}C$ values in the ocean is generally explained by the mixing of two end-members: refractory, aged DOC that is uniformly distributed in the water column and fresh, modern DOC produced in the surface layer (Mortazavi and Chanton 2004; Williams and Druffel 1987). In this ideal case, the distribution of $\Delta^{14}C$ values as a function of the inverse DOC concentrations ($[DOC]^{-1}$) is represented by a straight line in a Keeling plot (Beaupré and Aluwihare 2010; Keeling 1958; Mortazavi and Chanton 2004). This relationship is described by the following equation:

$$\Delta^{14}C_{\text{total}} = \left\{\left(\Delta^{14}C_{\text{refractory}} - \Delta^{14}C_{\text{fresh}}\right)[DOC]_{\text{refractory}}\right\}[DOC]_{\text{total}}^{-1} + \Delta^{14}C_{\text{fresh}} \quad (3)$$

In this case, the slope of the Keeling plot is the product of the (i) difference in the $\Delta^{14}C$ value between the refractory and fresh DOC end-members and (ii) the concentration of the refractory DOC end-member, while the y-intercept represents the $\Delta^{14}C$ value of the fresh DOC end-member. We used the Keeling plot to assess whether the model developed for open ocean environments is valid for this region and to identify the major DOC sources and potential removal processes in the system.

Results

Hydrography

The hydrography of the YS and ECS is affected primarily by the seasonal variability resulting from the mixing of the Kuroshio and coastal waters. In this study, to better understand the DOC characteristics in each region, we referred to the water mass classification of Chen (2009) and identified key water masses based on their temperature–salinity distributions. In detail, the Kuroshio-derived water mass entering the ECS was classified as Tsushima Warm Water (TWW), while coastal waters were categorized into three main types: Yellow Sea Warm Water (YSWW), Yellow Sea Cold Water (YSCW), and Changjiang Diluted Water (CDW) (Fig. 2).

TWW, which is a branch of the Kuroshio Current that flows into the ECS south of Jeju Island, is characterized by high temperature and high salinity (Chen 2009; Ichikawa and Beardsley 2002; Lie et al. 2000). CDW is a low-salinity (< 32) water mass formed by the mixing of ambient seawater and freshwater from the Changjiang River (Lie et al. 2003). In summer, it flows northeastward, reaching Jeju Island and the YS, whereas in winter it moves southward along the Chinese coast under the influence of the monsoon (Chang and Isobe 2003; Lie and Cho 2016). The seawater in the YS has a relatively long residence time of several years and undergoes mixing with groundwater and freshwater, as well as various biogeochemical processes, resulting in characteristics distinct from the other two water masses (Chen 2009; Kim et al. 2005). YSCW is formed by the mixing of YSWW and saline water of Kuroshio origin, which enters the YS from the southeast of Jeju Island in winter. During summer, YSCW remains in the bottom layer of the YS and moves gradually southward into the ECS (Lie et al. 2001).

In the YS, during summer (August 2020), the seawater temperature ranged from 8.8 to 28.2°C and salinity varied from 31.0 to 34.3 (Fig. 2). A thermocline formed at ~ 20 m depth (Supporting Information Fig. S1), with YSWW observed in the surface layer and YSCW in the bottom layer. In the central YS (Stas. #1–11), the temperature of YSCW below the thermocline increased southward (Supporting Information Fig. S1). Around the southern coast of the Korean Peninsula and the waters surrounding Jeju Island (Stas. #17–19), YSWW was present in the surface layer, and TWW in the bottom layer. In the ECS (Stas. #12–16 and #20–26; Fig. 1), the water masses

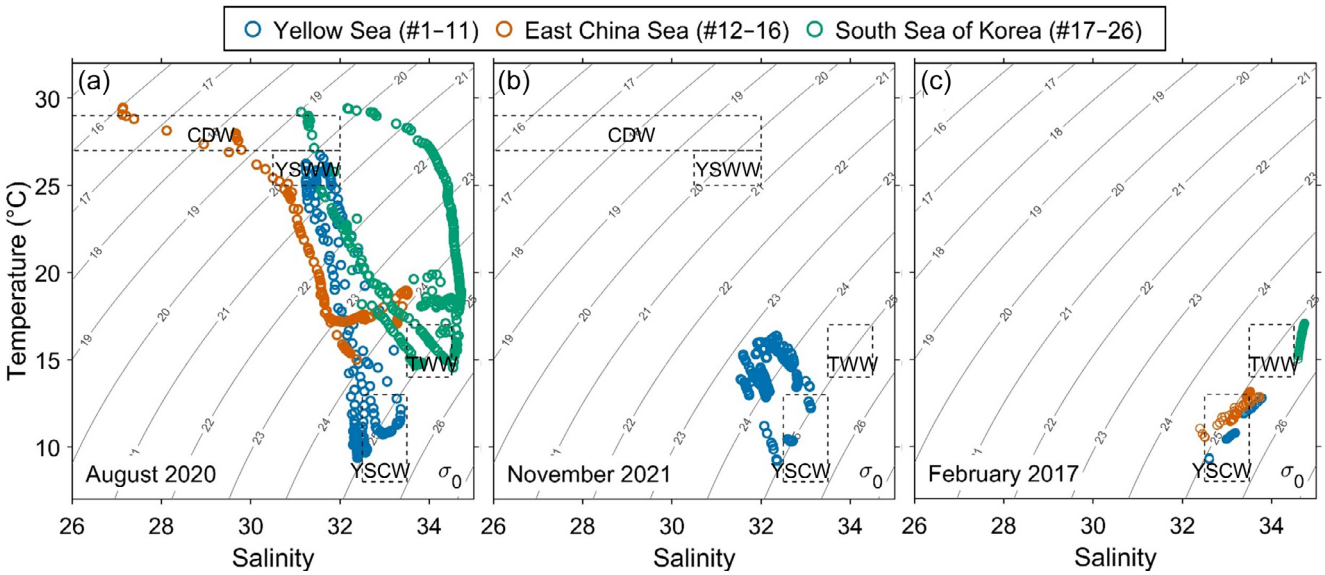

Fig. 2. Temperature–salinity diagrams for (**a**) August 2020, (**b**) November 2021, and (**c**) February 2017. The stations are grouped into three regions. Water masses are classified according to the scheme of Chen (2009) (CDW, Changjiang Diluted Water; YSWW, Yellow Sea Warm Water; YSCW, Yellow Sea Cold Water; TWW, Tsushima Warm Water). The contour lines are potential density anomalies (σ_0 = density – 1000 kg m^{-3}).

exhibited temperatures of 14.1–29.4°C and salinities of 26.7–34.7 (Fig. 2). At Sta. #16, CDW with a salinity of 27 was detected in the surface layer, reflecting the effect of the Changjiang River plume (Supporting Information Fig. S1). TWW was observed in the bottom layer of stations located south of the Korean Peninsula and Jeju Island (Stas. #20–26) (Fig. 2).

In the YS during autumn (November 2021), seawater temperature was 8.7–18.3°C and salinity was 31.5–33.8, exhibiting a much narrower range as compared with summer (Fig. 2). A significant temperature change was observed at ~ 40 m depth, and in the bottom layer the temperature increased southward. During winter (February 2017), seawater temperature in the YS and ECS was 9.2–17.1°C and the salinity was 32.4–34.7, having a relatively narrow range (Han et al. 2022). The water column was well mixed (Fig. 2 and Supporting Information Fig. S1). In the bottom layer of Stas. #10–12 (~ 33°N), temperature (13°C) and salinity (33.7) were higher than in the surface layer (Supporting Information Fig. S1). At the stations east of Jeju Island (Stas. #22–26), TWW with a salinity of > 34.5 was observed throughout the water column.

Distribution of DOC concentrations and Δ^{14}C values

During summer, DOC concentrations were 67–109 μM (mean 90 ± 13 μM; n = 11) in the surface layer, 72–98 μM (73 ± 12 μM; n = 11) in the middle layer, and 49–91 μM (69 ± 15 μM; n = 11) in the bottom layer (Fig. 3a). High DOC concentrations of > 100 μM were observed in the surface layer at Sta. #16, located in the southernmost ECS, and at Stas. #1 and #3 in the central YS. In contrast, low DOC concentrations of < 60 μM were found in the middle and bottom layers at Stas. #17, #21, #22, and #26, located to the southwest of the Korean Peninsula and south of Jeju Island. Overall, DOC concentrations were higher in the YS than in the ECS at comparable depths. DOC concentrations generally decreased with depth, with the highest values observed in the surface layer. However, at Sta. #3-2 the DOC concentration was higher in the bottom layer than in the mid-depth layer.

In autumn, DOC concentrations in the YS ranged from 70 to 93 μM (Fig. 3c). Similar to summer, high DOC concentrations of > 90 μM were observed in the central YS surface waters. However, compared with summer, the vertical variation in DOC concentrations was less pronounced and, at some stations, the expected decrease in DOC concentrations with depth was not clearly observed. In winter, DOC concentrations in the YS and ECS ranged from 52 to 97 μM (Fig. 3e) (Han et al. 2022). High DOC concentrations (88–97 μM) were observed at Sta. #6 in the northern YS, while the other stations had relatively stable concentrations of 52–77 μM. Overall, DOC concentrations decreased southward. The differences in DOC concentrations between the surface, middle, and bottom layers at most stations were within ±6 μM, except for Sta. #12.

In summer, DOC Δ^{14}C values ranged from −342‰ to −148‰ (Fig. 3b, d, and f), with a mean of −178‰ ± 26‰ (n = 9) in the surface layer, −216‰ ± 50‰ (n = 11) in the middle layer, and −238‰ ± 64‰ (n = 10) in the bottom layer. Similar to DOC concentrations, Δ^{14}C values decreased with depth. The highest Δ^{14}C values were observed in the central YS, while lower values of less than − 300‰ were found in the deep layers at Stas. #21, #22, and #26 off the southwestern

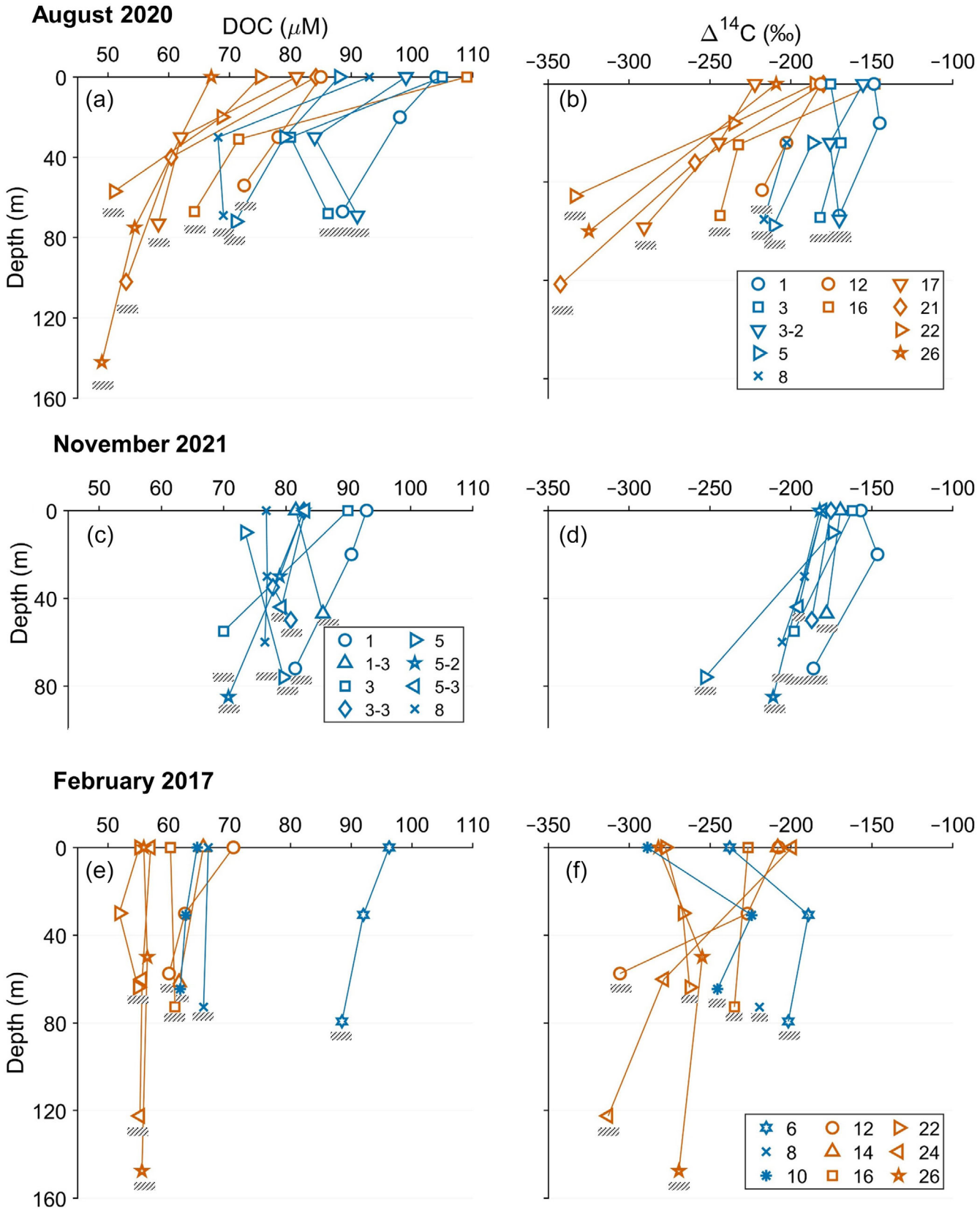

Fig. 3. Legend on next page.

Korean Peninsula. In contrast to the higher DOC concentrations in the mid-depth layers as compared with the bottom layers at Stas. #3-2 and #8, the lowest $\Delta^{14}C$ values were observed in the deep layers.

In autumn, DOC $\Delta^{14}C$ values in the YS ranged from −253‰ to −147‰ (Fig. 3d), with surface layer values ranging from −182‰ to −157‰ (−173‰ ± 9‰; $n = 8$). In the mid-depth and bottom layers, values ranged from −253‰ to −147‰ (−195‰ ± 28‰; $n = 10$), with lower values observed in these layers as compared with the surface. In winter, DOC $\Delta^{14}C$ values in the YS and ECS ranged from −289‰ to −189‰ (Fig. 3f) (Han et al. 2022). At Stas. #12, #16, and #24, $\Delta^{14}C$ values tended to decrease with depth, whereas at the other stations, higher values were observed in the bottom layer, or the values remained similar with depth.

Salinity exhibited negative correlations with DOC concentrations and $\Delta^{14}C$ values (Fig. 4). The DOC concentrations and $\Delta^{14}C$ values in the high-salinity TWW were similar to those in the subsurface layer (100–200 m) of the North Pacific (50–56 μM and −310‰ to−360‰; Druffel et al. 2019, 2021). In contrast, lower-salinity coastal waters were enriched with fresh DOC. In waters with a salinity of < 32, DOC concentrations and $\Delta^{14}C$ values (75–109 μM and −203‰ to −155‰) were higher than in surface waters of the open ocean (60–80 μM and −400‰ to −200‰; Druffel et al. 2019; Hansell et al. 2009).

The data of this study from the three seasons exhibited a linear relationship in the Keeling plot ($R^2 = 0.74$; $n = 70$; $p < 0.0001$) (Fig. 5). The fresh DOC $\Delta^{14}C$ value estimated using a model II linear regression (Sokal and Rohlf 1995) was +30‰ ± 16‰, which was similar to the $\Delta^{14}C$ values of surface DIC measured in the study area in August 2020 (−8‰ to +12‰; $n = 3$; measured in 2023; Sunmin Oh and Jeomshik Hwang, unpublished data). Applying the Keeling plot to seasonal data revealed a stronger linear relationship in summer ($R^2 = 0.90$; $n = 30$; $p < 0.0001$) than in autumn ($R^2 = 0.33$; $n = 18$; $p = 0.0128$) and winter ($R^2 = 0.36$; $n = 22$; $p = 0.0034$).

Discussion

Influence of water mass mixing on DOC distribution

In general, the difference in DOC concentrations and $\Delta^{14}C$ values between the surface and bottom layers decreased from summer to autumn to winter (Fig. 3). This is primarily due to vertical mixing and weakening of the seasonal mixed layer. In low-salinity coastal water masses, DOC concentrations and $\Delta^{14}C$ values were higher as compared with those in high-salinity water masses from the Northwestern Pacific.

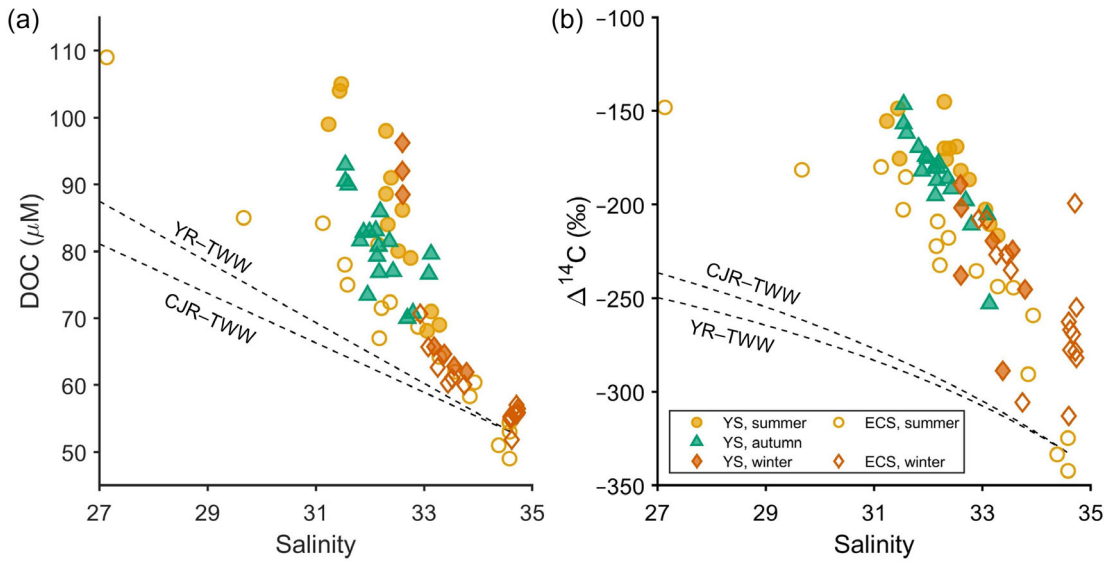

Fig. 4. Plots of salinity vs. (**a**) DOC concentrations and (**b**) DOC $\Delta^{14}C$ values for each season (August 2020, November 2021, and February 2017). The DOC data for summer and winter are divided by the sampling area (Yellow Sea and East China Sea). The dashed lines are mixing lines between Tsushima Warm Water (TWW) and the Yellow River (YR) and Changjiang River (CJR) in summer. The end-member values of the DOC concentrations and $\Delta^{14}C$ values for the Yellow River and Changjiang River are from Wang et al. (2012, 2016a) and Xue et al. (2017).

Fig. 3. Vertical distribution of (**a**, **c**, **e**) DOC concentrations and (**b**, **d**, **f**) $\Delta^{14}C$ values in the Yellow Sea (blue symbols) and East China Sea (red symbols) in August 2020, November 2021, and February 2017. The data for February 2017 are from Han et al. (2022). The lines connecting symbols are for visual guidance only, and are not interpolations. The bottom-water depth of each station is indicated by the black hatching. The numbers in the legends are station numbers.

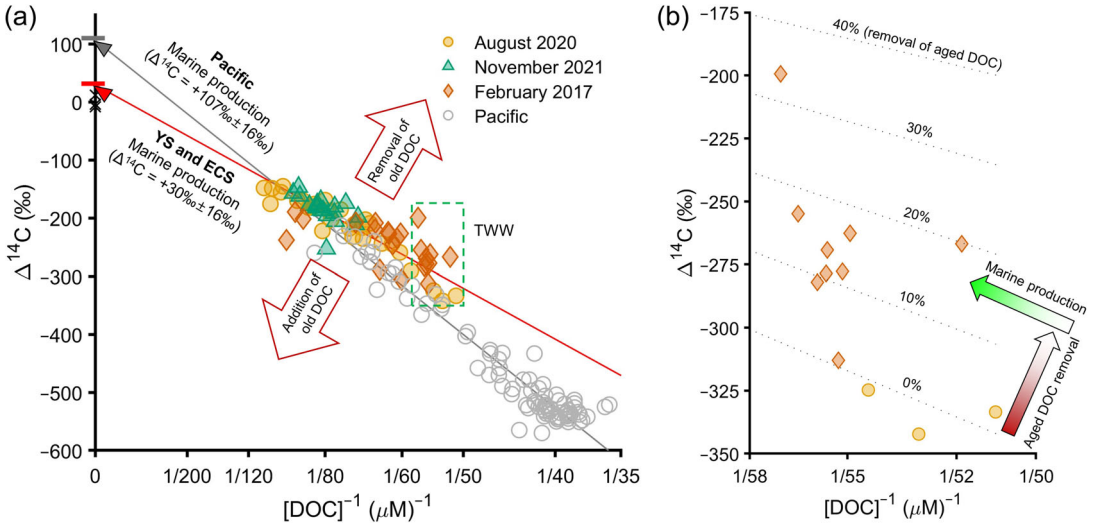

Fig. 5. (**a**) Keeling plot for the data collected during two cruises (August 2020 and November 2021), and the data for February 2017 (Han et al. 2022). For comparison, Pacific Ocean Data (P16 cruise along 150°W; Druffel et al. 2019) is also shown. A model II regression was used to estimate the *y*-intercept of the Keeling plot (Mortazavi and Chanton 2004), and the *y*-intercepts of each regression line are shown. The black × symbols on the *y*-axis are the surface DIC $\Delta^{14}C$ values for the Yellow Sea and East China Sea in August 2020 (Sunmin Oh and Jeomshik Hwang, unpublished data). The green dashed rectangle highlights the data corresponding to Tsushima Warm Water (TWW). (**b**) Close-up view of the TWW DOC data as indicated by the dashed rectangle in (**a**), including both summer and winter observations. The dashed lines denote the removal of refractory DOC in per cent from the summer end-member (indicated as 0%).

In summer, coastal water masses and water masses from the open ocean formed a stratified structure, with a clear trend of decreasing DOC concentrations and $\Delta^{14}C$ values from the sea surface to bottom. As the seasons transitioned to autumn and winter, the decrease in surface water temperature and freshwater discharge and stronger winds enhanced vertical mixing, leading to a decrease in the differences in DOC concentrations and $\Delta^{14}C$ values with depth.

The DOC concentrations and $\Delta^{14}C$ values in the present study area were significantly higher than what would result from conservative mixing of DOC between TWW and freshwater from the Yellow River or Changjiang River (Fig. 4), indicating that a substantial amount of DOC is produced in this region. Previous studies have suggested that terrestrial DOC entering an estuary through rivers is rapidly decomposed due to priming (Bianchi 2011). For example, Xue et al. (2017) found that, as salinity increased from 0 to 30 over a distance of ~ 20 km in the Yellow River Estuary, DOC $\delta^{13}C$ values changed rapidly to marine biogenic values. The vertically generalized production model (VGPM) (Behrenfeld and Falkowski 1997) showed that net primary production near the Changjiang River exceeded 1000 g C m^{-2} yr^{-1}, demonstrating the effect of freshwater input on marine primary production (Supporting Information Fig. S2). The increase in DOC concentrations may have been driven by enhanced marine primary production due to nutrient supply from land and/or remineralization of terrestrial DOC or POC (Kim et al. 2020).

The DOC concentrations and $\Delta^{14}C$ values in the YS were higher in the salinity range of 30–33 as compared with the ECS (Fig. 4). This can be attributed to the proximity of the YS to the continent, which resulted in less dilution from low-DOC oceanic sources, as well as higher primary production in the YS as compared with the ECS, and the potential influx of DOC from sources such as groundwater or sediments during the water residence time of a few years (Han et al. 2022; Ji et al. 2024; Kim et al. 2005; Seo et al. 2022). The differences in the relationship between DOC concentrations or $\Delta^{14}C$ values and salinity suggest that the addition and removal of DOC from various sources with differing $\Delta^{14}C$ values occur during water mass mixing. Seasonally, scatter in the relationship between $\Delta^{14}C$ values and salinity was more pronounced in winter than in summer. In the ECS and off the southern coast of Korea, the DOC distribution in summer reflects mixing between the surface and bottom layers. However, in winter, DOC concentrations were similar between the surface and bottom waters, but significant vertical differences in $\Delta^{14}C$ values were observed. Intensified wind-induced vertical mixing in winter could enhance sediment resuspension (Bian et al. 2013), and the addition of aged DOC from disintegration of resuspended sediment near the seafloor may have caused the observed vertical distribution of $\Delta^{14}C$.

In the region where Kuroshio-derived TWW was dominant, the mean DOC concentration in the TWW layer in winter was 2 μM higher than that in summer, while the $\Delta^{14}C$ value was ~ 70‰ higher (Fig. 4). The apparent oxygen utilization (AOU) value of TWW in summer was ~ 86 μmol kg^{-1}, significantly higher than in winter (< 20 μmol kg^{-1}) (Supporting Information Fig. S3). Low DOC concentration with low AOU in

summer TWW than in winter implies that net remineralization of organic matter occurred as the Kuroshio-derived water entered the ECS during summer. Labile DOC that forms primarily by marine primary production would have a modern $\Delta^{14}C$ value. As this labile DOC is removed, the $\Delta^{14}C$ value of total DOC decreases, and AOU increases.

Identifying the processes affecting the DOC concentrations and $\Delta^{14}C$ values

The DOC $\Delta^{14}C$ values in the YS and ECS ranging from −145‰ to −342‰ correspond to ^{14}C ages of 1200–3300 yr BP. Considering that the water residence time in the study area is only a few years (Kim et al. 2005; Nozaki et al. 1991), this suggests that DOC older than 1000 yr is being introduced into these regions. The average depth of the ECS, including the continental slope, is 370 m, at which depth the $\Delta^{14}C$ value of North Pacific DOC is −390‰ ± 57‰ (DOC data from the P16 cruise; Druffel et al. 2019). Thus, the presence of millennial-aged DOC in regions with residence times of only a few years implies an external source, with the North Pacific serving as a likely supplier of aged DOC.

The DOC concentration and $\Delta^{14}C$ distribution in the YS and ECS were aligned on a straight line in the Keeling plot. This suggests that DOC cycling in these marginal seas can also be explained by a two-component model, similar to that of the open ocean. Radiocarbon study conducted in the East Sea (Japan Sea), which is another marginal sea connected with the Northwestern Pacific, implied that aged, refractory DOC in the Northwestern Pacific is transported into the East Sea (Japan Sea) via shallow straits without significant degradation (Ryu et al. 2023). Thus, we assume that a major portion of aged DOC is derived from the Northwestern Pacific. Also, this further confirms that marine primary production was the dominant source of DOC in these marginal seas. In the open ocean, 30–50% of the net primary production is converted into DOC, most of which consists of labile DOC that is decomposed by microbes within hours to days, leaving < 10% of the initially produced DOC to persist in the ocean for more than several months (Hansell 2013). The annual primary production in the YS and ECS is 145 g C m^{-2} yr^{-1} (Gong et al. 2003). Assuming that 10% of the primary production was released as DOC and was uniformly distributed within a 20 m water column, annual DOC accumulation of 50 μmol C L^{-1} yr^{-1} would be expected. The observed difference in surface DOC concentrations between summer and winter was ∼ 24 μM, which is consistent with the expected accumulation of DOC from marine primary production over 6 months (August–February).

It appears that the slope is less steep for this region than for the open ocean (Fig. 5). We suspect that two factors were responsible for the difference. One is that the DIC $\Delta^{14}C$ value, which determines the $\Delta^{14}C$ value of the freshly produced DOC, was lower in the study region (−8‰ to + 12‰) than in the North Pacific (∼ 30‰; Ge et al. 2022). The other is the removal of aged DOC, which is further discussed below.

The weaker linear relationships in autumn and winter than in summer can be attributed not only to the narrower data range but also the effect of scatter about the expected linear trend. When aged DOC is introduced in addition to the two end-member DOC components, the resulting divergence is to the lower left in the Keeling plot, whereas the decomposition of aged DOC causes divergence toward the upper right (indicated by arrows in Fig. 5). In contrast, the addition and removal of fresh DOC moves data points along the regression line without causing divergence. Similar to the DOC distribution with respect to salinity, the divergences in the Keeling plot also indicate that there were additional DOC sources in autumn and winter beyond primary production.

The $\Delta^{14}C$ values of DOC in TWW in summer and winter exhibit a clear difference, with winter samples plotting to the upper right on the Keeling plot as compared with summer samples (Fig. 5). This distribution suggests that the observed changes of DOC in TWW cannot be solely explained by the addition of fresh DOC. The observed data can be explained by a combination of the removal of aged DOC and the production of fresh DOC (brown and green arrows, respectively, in Fig. 5b). The removal of this refractory DOC may be attributed to the combined effects of microbial consumption and photochemical degradation. Supporting evidence comes from observations in the inner bay of the Amundsen Sea, Antarctica, where the degradation of old, refractory DOC was conjectured during polynya opening based on $\Delta^{14}C$ results (Fang et al. 2020). This process appears to be driven by the addition of high concentrations of fresh DOC derived from phytoplankton blooms, which stimulate the removal of aged DOC. If the lowest DOC concentrations and $\Delta^{14}C$ values observed in summer TWW are considered representative of the refractory DOC end-member, the fraction of refractory DOC removed (α) can be estimated using the following mass balance equation:

$$\begin{aligned}&\left([DOC]_{RDOC}-\alpha\right)\Delta^{14}C_{RDOC}\\&+\left([DOC]_{total}-[DOC]_{RDOC}-\alpha\right)\Delta^{14}C_{fresh}\\&=[DOC]_{total}\Delta^{14}C_{total}\end{aligned}\quad(4)$$

where RDOC denotes refractory DOC.

Assuming the refractory DOC pool is uniform with respect to $\Delta^{14}C$ and that the added fresh DOC has the $\Delta^{14}C$ value of surface water DIC in this region, the estimated removal of refractory DOC in winter TWW is 10–30% of the total DOC (Fig. 5b). This finding suggests that marine refractory DOC can be actively removed on the continental shelf.

Potential sources of DOC in the Yellow Sea and East China Sea

Contributions from various sources, including allochthonous DOC transported from boundary regions, appear to result in greater $\Delta^{14}C$ scatter in the Keeling plot as compared with the

open ocean. We examined the flux of potential DOC sources and their influence on the DOC pool. The Changjiang River and Yellow River supply DOC into the ECS and YS with $\Delta^{14}C$ values of −183‰ to −44‰ and −195‰ to −158‰, respectively, at annual fluxes of 1.6 and 0.03 Tg C, respectively (Wang et al. 2012, 2016a; Xue et al. 2017). In addition, major rivers of the Korean Peninsula (the Han, Geum, Youngsan, and Sumjin rivers) contribute 0.08–0.09 Tg C of DOC annually to the YS and ECS, with a mean $\Delta^{14}C$ value of −26‰ (− 124‰ to 1‰) (Lee et al. 2021). The total contribution of these rivers (~ 2 Tg C yr^{-1}) accounts for ~ 10% of the total DOC pool in the YS and ECS (2.85×10^{14} $m^3 \times 60\ \mu M + 1.7 \times 10^{13}$ $m^3 \times 80\ \mu M = \sim 20$ Tg C) and about 1% of the total primary production (~ 170 Tg C; estimated from the values reported by Gong et al. 2003, and the surface area of the study region). Interestingly, despite the highest freshwater discharge occurring in summer, the Keeling plot exhibited the least scatter during this season. This suggests that terrestrially derived DOC is rapidly degraded in estuaries, limiting its contribution to the observed DOC scatter in the study region.

According to Ren et al. (2022), aerosol POC deposited in the Bohai Sea is derived primarily from fossil fuel combustion, with a high proportion of black carbon. In winter, the contribution of fossil carbon increases, resulting in low $\Delta^{14}C$ values of aerosol POC (−304‰ to −640‰). Yu et al. (2018) reported seasonal $\Delta^{14}C$ values of aerosols collected from Changdao, Qingdao, and Huaniao Island, and estimated that ~ 1.3 Tg C from fossil carbon was annually deposited into the YS and ECS. This aerosol-derived POC can contribute to the aged DOC pool if degraded to DOC. However, since most POC that enters the water column is known to settle and accumulate in sediments (Bao et al. 2016; Ren et al. 2022), its overall effect on the DOC distribution is likely to be limited. Although the $\Delta^{14}C$ values of wet deposition of DOC in the YS and ECS are not well documented, $\Delta^{14}C$ values of DOC in rain collected in Seoul, South Korea, and coastal cities in China (Qingdao and Yantai), range widely from −23‰ to −483‰ (Wang et al. 2016b; Yan and Kim 2017). The wet deposition flux of DOC has been estimated to vary from 1.90 to 3.15 g C m^{-2} yr^{-1} in Seoul and Jiaozhou Bay, located in the western YS (Xing et al. 2019; Yan and Kim 2012). If this flux is applied to the whole area of the YS and ECS, the annual DOC input from rainfall is estimated to be 2.2–3.6 Tg C yr^{-1}, comparable to the amount supplied by riverine input.

In the study area, the mean concentration of suspended POC (0.8–51 μm particle size) in the water column in summer was $4 \pm 3\ \mu M$, which is > 10 times higher than that in the surface waters of the open ocean, with $\Delta^{14}C$ values ranging from −312‰ to −28‰ (Seo et al. 2022). The $\Delta^{14}C$ values of suspended POC in the surface layer averaged −90‰ (−146‰ to −28‰), lower than the surface DIC $\Delta^{14}C$ values, and decreased with depth, reaching an average of −240‰ near the seafloor (Seo et al. 2022). Degradation of suspended POC into DOC could reduce the DOC $\Delta^{14}C$ values (Smith et al. 1992). During winter, when vertical mixing is stronger, the resuspension of sedimentary POC from the seafloor may introduce DOC with $\Delta^{14}C$ values lower than −300‰ into surface waters. However, DOC could also be removed through adsorption onto suspended POC (Druffel and Williams 1990; Hwang et al. 2006). An assessment of the quantitative effect of suspended POC on the overall DOC pool is not currently possible.

Another source of DOC is the supply from sediments. Porewater DOC concentrations in the surface sediments (0–2 cm) of the YS and ECS have been reported to range from 2.5 to 5.6 mM, with $\Delta^{14}C$ values between −66‰ and −12‰ (Fu et al. 2022). These $\Delta^{14}C$ values are considerably higher than those of POC in surface sediments (−364‰ to −290‰; Bao et al. 2016), suggesting that more recently produced POC is selectively degraded to DOC (Fu et al. 2022). Given that porewater DOC concentrations are an order of magnitude higher than those in the bottom water, porewater DOC would diffuse to the overlying water column (Komada et al. 2013). The vertical benthic flux due to diffusion was estimated using Fick's first law (Ingall et al. 2005) as follows:

$$F = -\phi D_{\text{sed}} \left(\frac{\partial C}{\partial z} \right)_{z=0} \quad (5)$$

where F represents the benthic diffusion flux, ϕ is the porosity, D_{sed} is the diffusion coefficient in porewater, and $(\partial C/\partial z)_{z=0}$ is the DOC concentration gradient across the sediment–water interface. Using the porewater DOC concentrations in surface sediments (Fu et al. 2022; 2.5–5.6 mM), the average bottom-water (~ 3 m above the ocean floor) DOC concentration (in this study = $70 \pm 13\ \mu M$), $\phi = 0.8$ (for silt; Zhou et al. 2022), and D_{sed} = 0.2–0.6 cm^2 d^{-1} (Balch and Guéguen 2015), the estimated benthic diffusion flux of DOC is 5–32 mmol DOC m^{-2} yr^{-1}. This corresponds to 0.1–0.4 Tg C yr^{-1}, which is higher than the DOC flux from the Yellow River (0.03 Tg DOC yr^{-1}; Wang et al. 2012) and Korean rivers (0.08–0.09 Tg C yr^{-1}; Lee et al. 2021). As such, porewater DOC could be a significant source of fresh DOC in the bottom layer. However, this flux is considerably smaller than the primary production of 170 Tg C yr^{-1}. In addition, since the $\Delta^{14}C$ values were only slightly lower than those of DOC produced by primary production (Supporting Information Fig. S4), this would not cause considerable scatter in the Keeling plot. Overall, considering the magnitudes of each potential source, primary production of 170 Tg C yr^{-1}, atmospheric wet deposition of 2.2–3.6 Tg C yr^{-1}, river input of ~ 2 Tg C yr^{-1}, pore-water diffusion of 0.1–0.4 Tg C yr^{-1}, marine primary production appears by far the largest source of DOC. However, $\Delta^{14}C$ value-wise, each source can affect $\Delta^{14}C$ value of DOC disproportionally depending on their $\Delta^{14}C$ values, causing scatters in the Keeling plot.

Author Contributions

Yeongjin Ryu designed the research, conducted field sampling, performed radiocarbon analysis, and wrote the manuscript;

Heejun Han analyzed DOC concentrations; Taehee Na conducted field sampling and performed radiocarbon measurements; Guebuem Kim supervised the research and contributed to writing; Jeomshik Hwang supervised the research, guided data interpretation, and contributed to writing.

Acknowledgments

We thank the captain and crew of the RV *Onnuri* for their support during sample collection and hydrographic observations at sea, and the staff at the NOSAMS (WHOI) and Keck Carbon Cycle Facility at UC Irvine for the carbon isotope analyses. This research was supported by the Mid-Career Bridging Program of Seoul National University, the National Research Foundation of Korea (NRF) grant funded by the Korean government (MSIT) (RS-2023-00208830), and the Korea Institute of Marine Science & Technology Promotion (KIMST) grant funded by the Ministry of Oceans and Fisheries, Korea (20220541, Changes in the physical and biogeochemical environment in the Tsushima Warm Current system of Korean Waters).

Conflicts of Interest

None declared.

Data Availability Statement

All data supporting the results of this study are provided in the Supporting Information.

References

Balch, J., and C. Guéguen. 2015. "Determination of Diffusion Coefficients of Dissolved Organic Matter in the Churchill River Estuary System, Hudson Bay (Canada)." *Environment and Chemistry* 12, no. 2: 253–260. https://doi.org/10.1071/EN14182.

Bao, R., C. McIntyre, M. X. Zhao, C. Zhu, S. J. Kao, and T. I. Eglinton. 2016. "Widespread Dispersal and Aging of Organic Carbon in Shallow Marginal Seas." *Geology* 44, no. 10: 791–794. https://doi.org/10.1130/G37948.1.

Bauer, J., and T. Bianchi. 2011. "Dissolved Organic Carbon Cycling and Transformation." In Treatise on Estuarine and Coastal Science, edited by E. Wolanski and D. McLusky, 7–67. Academic Press.

Bauer, J. E., W. J. Cai, P. A. Raymond, T. S. Bianchi, C. S. Hopkinson, and P. A. G. Regnier. 2013. "The Changing Carbon Cycle of the Coastal Ocean." *Nature* 504: 61–70. https://doi.org/10.1038/nature12857.

Bauer, J. E., E. R. M. Druffel, D. M. Wolgast, and S. Griffin. 2002. "Temporal and Regional Variability in Sources and Cycling of DOC and POC in the Northwest Atlantic Continental Shelf and Slope." *Deep-Sea Research Part II: Topical Studies in Oceanography* 49, no. 20: 4387–4419. https://doi.org/10.1016/S0967-0645(02)00123-6.

Bauer, J. E., P. M. Williams, and E. R. M. Druffel. 1992. "C-14 Activity of Dissolved Organic-Carbon Fractions in the North-Central Pacific and Sargasso Sea." *Nature* 357: 667–670. https://doi.org/10.1038/357667a0.

Beaupré, S. R., and L. Aluwihare. 2010. "Constraining the 2-Component Model of Marine Dissolved Organic Radiocarbon." *Deep-Sea Research Part II: Topical Studies in Oceanography* 57, no. 16: 1494–1503. https://doi.org/10.1016/j.dsr2.2010.02.017.

Beaupré, S. R., E. R. M. Druffel, and S. Griffin. 2007. "A Low-Blank Photochemical Extraction System for Concentration and Isotopic Analyses of Marine Dissolved Organic Carbon." *Limnology and Oceanography: Methods* 5, no. 6: 174–184. https://doi.org/10.4319/lom.2007.5.174.

Behrenfeld, M. J., and P. G. Falkowski. 1997. "Photosynthetic Rates Derived from Satellite-Based Chlorophyll Concentration." *Limnology and Oceanography* 42, no. 1: 1–20. https://doi.org/10.4319/lo.1997.42.1.0001.

Bian, C., W. Jiang, Q. Quan, T. Wang, R. J. Greatbatch, and W. Li. 2013. "Distributions of Suspended Sediment Concentration in the Yellow Sea and the East China Sea Based on Field Surveys during the Four Seasons of 2011." *Journal of Marine Systems* 121: 24–35. https://doi.org/10.1016/j.jmarsys.2013.03.013.

Bianchi, T. S. 2011. "The Role of Terrestrially Derived Organic Carbon in the Coastal Ocean: A Changing Paradigm and the Priming Effect." *Proceedings of the National Academy of Sciences of the United States of America* 108, no. 49: 19473–19481. https://doi.org/10.1073/pnas.1017982108.

Butman, D. E., H. F. Wilson, R. T. Barnes, M. A. Xenopoulos, and P. A. Raymond. 2015. "Increased Mobilization of Aged Carbon to Rivers by Human Disturbance." *Nature Geoscience* 8: 112–116. https://doi.org/10.1038/ngeo2322.

Chang, P. H., and A. Isobe. 2003. "A Numerical Study on the Changjiang Diluted Water in the Yellow and East China Seas." *Journal of Geophysical Research: Oceans* 108, no. C9: 1–17. https://doi.org/10.1029/2002JC001749.

Chen, C. T. A. 2009. "Chemical and Physical Fronts in the Bohai, Yellow and East China Seas." *Journal of Marine Systems* 78, no. 3: 394–410. https://doi.org/10.1016/j.jmarsys.2008.11.016.

Chen, X. G., F. F. Zhang, Y. L. Lao, X. L. Wang, J. Z. Du, and I. R. Santos. 2018. "Submarine Groundwater Discharge-Derived Carbon Fluxes in Mangroves: An Important Component of Blue Carbon Budgets?" *Journal of Geophysical Research: Oceans* 123, no. 9: 6962–6979. https://doi.org/10.1029/2018JC014448.

Druffel, E. R. M., S. Griffin, A. I. Coppola, and B. D. Walker. 2016. "Radiocarbon in Dissolved Organic Carbon of the Atlantic Ocean." *Geophysical Research Letters* 43, no. 10: 5279–5286. https://doi.org/10.1002/2016GL068746.

Druffel, E. R. M., S. Griffin, C. B. Lewis, et al. 2021. "Dissolved Organic Radiocarbon in the Eastern Pacific and Southern

Oceans." *Geophysical Research Letters* 48, no. 10: e2021GL092904. https://doi.org/10.1029/2021GL092904.

Druffel, E. R. M., S. Griffin, N. Wang, et al. 2019. "Dissolved Organic Radiocarbon in the Central Pacific Ocean." *Geophysical Research Letters* 46, no. 10: 5396–5403. https://doi.org/10.1029/2019GL083149.

Druffel, E. R. M., and P. M. Williams. 1990. "Identification of a Deep Marine Source of Particulate Organic-Carbon Using Bomb C-14." *Nature* 347: 172–174. https://doi.org/10.1038/347172a0.

Druffel, E. R. M., P. M. Williams, J. E. Bauer, and J. R. Ertel. 1992. "Cycling of Dissolved and Particulate Organic-Matter in the Open Ocean." *Journal of Geophysical Research: Oceans* 97, no. C10: 15639–15659. https://doi.org/10.1029/92JC01511.

Fang, L., S. H. Lee, S.-A. Lee, et al. 2020. "Removal of Refractory Dissolved Organic Carbon in the Amundsen Sea, Antarctica." *Scientific Reports* 10: 1213. https://doi.org/10.1038/s41598-020-57870-6.

Fu, W. J., W. Fu, X. Xu, et al. 2022. "Carbon Isotopic Constraints on the Degradation and Sequestration of Organic Matter in River-Influenced Marginal Sea Sediments." *Limnology and Oceanography* 67, no. S2: S61–S75. https://doi.org/10.1002/lno.12070.

Ge, T. T., C. Luo, P. Ren, et al. 2022. "Decadal Variations in Radiocarbon in Dissolved Inorganic Carbon (DIC) Along a Transect in the Western North Pacific Ocean." *Journal of Geophysical Research: Oceans* 127, no. 2: e2021JC017845. https://doi.org/10.1029/2021JC017845.

Gong, G. C., Y. H. Wen, B. W. Wang, and G. J. Liu. 2003. "Seasonal Variation of Chlorophyll *a* Concentration, Primary Production and Environmental Conditions in the Subtropical East China Sea." *Deep-Sea Research Part II: Topical Studies in Oceanography* 50, no. 6–7: 1219–1236. https://doi.org/10.1016/S0967-0645(03)00019-5.

Guo, L. D., P. H. Santschi, L. A. Cifuentes, S. E. Trumbore, and J. Southon. 1996. "Cycling of High-Molecular-Weight Dissolved Organic Matter in the Middle Atlantic Bight as Revealed by Carbon Isotopic (C-13 and C-14) Signatures." *Limnology and Oceanography* 41, no. 6: 1242–1252. https://doi.org/10.4319/lo.1996.41.6.1242.

Halewood, E., K. Opalk, L. Custals, M. Carey, D. A. Hansell, and C. A. Carlson. 2022. "Determination of Dissolved Organic Carbon and Total Dissolved Nitrogen in Seawater Using High Temperature Combustion Analysis." *Frontiers in Marine Science* 9: 1061646. https://doi.org/10.3389/fmars.2022.1061646.

Han, H., T. Na, H. M. Cho, G. Kim, and J. Hwang. 2022. "Large Fluxes of Continental-Shelf-Borne Dissolved Organic Carbon in the East China Sea and the Yellow Sea." *Marine Chemistry* 240: 104097. https://doi.org/10.1016/j.marchem.2022.104097.

Hansell, D. A. 2013. "Recalcitrant Dissolved Organic Carbon Fractions." *Annual Review of Marine Science* 5: 421–445. https://doi.org/10.1146/annurev-marine-120710-100757.

Hansell, D. A., and C. A. Carlson. 1998. "Deep-Ocean Gradients in the Concentration of Dissolved Organic Carbon." *Nature* 395: 263–266. https://doi.org/10.1038/26200.

Hansell, D. A., C. A. Carlson, D. J. Repeta, and R. Schlitzer. 2009. "Dissolved Organic Matter in the Ocean a Controversy Stimulates New Insights." *Oceanography* 22, no. 4: 202–211. https://doi.org/10.5670/oceanog.2009.109.

Hedges, J. I., and R. G. Keil. 1995. "Sedimentary Organic-Matter Preservation—An Assessment and Speculative Synthesis." *Marine Chemistry* 49, no. 2–3: 81–115. https://doi.org/10.1016/0304-4203(95)00008-F.

Hwang, J., and E. R. M. Druffel. 2005. "Blank Correction for Δ14C Measurements in Organic Compound Classes of Oceanic Particulate Matter." *Radiocarbon* 47, no. 1: 75–87. https://doi.org/10.1017/S0033822200052218.

Hwang, J. S., E. R. M. Druffel, and J. E. Bauer. 2006. "Incorporation of Aged Dissolved Organic Carbon (DOC) by Oceanic Particulate Organic Carbon (POC): An Experimental Approach Using Natural Carbon Isotopes." *Marine Chemistry* 98, no. 2–4: 315–322. https://doi.org/10.1016/j.marchem.2005.10.008.

Ichikawa, H., and R. C. Beardsley. 2002. "The Current System in the Yellow and East China Seas." *Journal of Oceanography* 58: 77–92. https://doi.org/10.1023/A:1015876701363.

Ingall, E., L. Kolowith, T. Lyons, and M. Hurtgen. 2005. "Sediment Carbon, Nitrogen and Phosphorus Cycling in an Anoxic Fjord, Effingham Inlet, British Columbia." *American Journal of Science* 305, no. 3: 240–258. https://doi.org/10.2475/ajs.305.3.240.

Ji, X., M.-L. Zhao, J. Zhang, and G.-P. Yang. 2024. "Spatial Variation in the Optical and Molecular Properties of Dissolved Organic Matter in the Yellow Sea and East China Sea." *Progress in Oceanography* 220: 103192. https://doi.org/10.1016/j.pocean.2023.103192.

Keeling, C. D. 1958. "The Concentration and Isotopic Abundances of Atmospheric Carbon Dioxide in Rural Areas." *Geochimica et Cosmochimica Acta* 13: 322–334. https://doi.org/10.1016/0016-7037(58)90033-4.

Kim, G., J. W. Ryu, H. S. Yang, and S. T. Yun. 2005. "Submarine Groundwater Discharge (SGD) into the Yellow Sea Revealed by 228Ra and 226Ra Isotopes: Implications for Global Silicate Fluxes." *Earth and Planetary Science Letters* 237, no. 1–2: 156–166. https://doi.org/10.1016/j.epsl.2005.06.011.

Kim, J., T. H. Kim, S. R. Park, H. J. Lee, and J. K. Kim. 2020. "Factors Controlling the Distributions of Dissolved Organic Matter in the East China Sea During Summer." *Scientific Reports* 10: 11854. https://doi.org/10.1038/s41598-020-68863-w.

Komada, T., D. J. Burdige, S. M. Crispo, et al. 2013. "Dissolved Organic Carbon Dynamics in Anaerobic Sediments of the Santa Monica Basin." *Geochimica et Cosmochimica Acta* 110: 253–273. https://doi.org/10.1016/j.gca.2013.02.017.

Kwon, E. Y., T. DeVries, E. D. Galbraith, J. Hwang, G. Kim, and A. Timmermann. 2021. "Stable Carbon Isotopes Suggest

Large Terrestrial Carbon Inputs to the Global Ocean." *Global Biogeochemical Cycles* 35, no. 4: e2020GB006684. https://doi.org/10.1029/2020GB006684.

Lee, E. J., Y. Shin, G.-Y. Yoo, et al. 2021. "Loads and Ages of Carbon From the Five Largest Rivers in South Korea Under Asian Monsoon Climates." *Journal of Hydrology* 599: 126363. https://doi.org/10.1016/j.jhydrol.2021.126363.

Lie, H. J., and C. H. Cho. 2016. "Seasonal Circulation Patterns of the Yellow and East China Seas Derived from Satellite-Tracked Drifter Trajectories and Hydrographic Observations." *Progress in Oceanography* 146: 121–141. https://doi.org/10.1016/j.pocean.2016.06.004.

Lie, H. J., C. H. Cho, J. H. Lee, and S. Lee. 2003. "Structure and Eastward Extension of the Changjiang River Plume in the East China Sea." *Journal of Geophysical Research. Oceans* 108, no. C3: 3077. https://doi.org/10.1029/2001JC001194.

Lie, H. J., C. H. Cho, J. H. Lee, S. Lee, and Y. X. Tang. 2000. "Seasonal Variation of the Cheju Warm Current in the Northern East China Sea." *Journal of Oceanography* 56: 197–211. https://doi.org/10.1023/A:1011139313988.

Lie, H. J., C. H. Cho, J. H. Lee, S. Lee, Y. X. Tang, and E. M. Zou. 2001. "Does the Yellow Sea Warm Current Really Exist as a Persistent Mean Flow?" *Journal of Geophysical Research. Oceans* 106: 22199–22210. https://doi.org/10.1029/2000JC000629.

Liu, M., P. A. Raymond, R. Lauerwald, et al. 2024. "Global Riverine Land-to-Ocean Carbon Export Constrained by Observations and Multi-Model Assessment." *Nature Geoscience* 17: 896–904. https://doi.org/10.1038/s41561-024-01524-z.

Lønborg, C., C. Carreira, T. Jickells, and X. A. Alvarez-Salgado. 2020. "Impacts of Global Change on Ocean Dissolved Organic Carbon (DOC) Cycling." *Frontiers in Marine Science* 7: 466. https://doi.org/10.3389/fmars.2020.00466.

McNichol, A. P., and L. I. Aluwihare. 2007. "The Power of Radiocarbon in Biogeochemical Studies of the Marine Carbon Cycle: Insights From Studies of Dissolved and Particulate Organic Carbon (DOC and POC)." *Chemical Reviews* 107: 443–466. https://doi.org/10.1021/cr050374g.

Meybeck, M. 1982. "Carbon, Nitrogen, and Phosphorus Transport by World Rivers." *American Journal of Science* 282: 401–450. https://doi.org/10.2475/ajs.282.4.401.

Mortazavi, B., and J. P. Chanton. 2004. "Use of Keeling Plots to Determine Sources of Dissolved Organic Carbon in Nearshore and Open Ocean Systems." *Limnology and Oceanography* 49, no. 1: 102–108. https://doi.org/10.4319/lo.2004.49.1.0102.

Nozaki, Y., H. Tsubota, V. Kasemsupaya, M. Yashima, and N. Ikuta. 1991. "Residence Times of Surface-Water and Particle-Reactive PB-210 and PO-210 in the East China and Yellow Seas." *Geochimica et Cosmochimica Acta* 55, no. 5: 1265–1272. https://doi.org/10.1016/0016-7037(91)90305-O.

Opsahl, S., and R. Benner. 1997. "Distribution and Cycling of Terrigenous Dissolved Organic Matter in the Ocean." *Nature* 386: 480–482. https://doi.org/10.1038/386480a0.

Ren, P., C. L. Luo, H. M. Zhang, H. Schiebel, M. G. Hastings, and X. C. Wang. 2022. "Atmospheric Particles Are Major Sources of Aged Anthropogenic Organic Carbon in Marginal Seas." *Environmental Science & Technology* 56, no. 19: 14198–14207. https://doi.org/10.1021/acs.est.2c06321.

Ryu, Y., H. Han, T. Na, G. Kim, E. R. M. Druffel, and J. Hwang. 2023. "Transport of Aged Dissolved Organic Carbon Via the Surface Current Revealed by Radiocarbon." *Geophysical Research Letters* 50, no. 22: e2023GL105296. https://doi.org/10.1029/2023GL105296.

Seo, J., G. Kim, and J. Hwang. 2022. "Sources and Behavior of Particulate Organic Carbon in the Yellow Sea and the East China Sea Based on 13C, 14C, and 234Th." *Frontiers in Marine Science* 9: 793556. https://doi.org/10.3389/fmars.2022.793556.

Shen, Y., and R. Benner. 2018. "Mixing it up in the Ocean Carbon Cycle and the Removal of Refractory Dissolved Organic Carbon." *Scientific Reports* 8: 2542. https://doi.org/10.1038/s41598-018-20857-5.

Smith, D. C., M. Simon, A. L. Alldredge, and F. Azam. 1992. "Intense Hydrolytic Enzyme-Activity on Marine Aggregates and Implications for Rapid Particle Dissolution." *Nature* 359: 139–142. https://doi.org/10.1038/359139a0.

Sokal, R. R., and F. J. Rohlf. 1995. Biometry. Macmillan.

Stuiver, M., and H. A. Polach. 1977. "Reporting of C-14 Data—Discussion." *Radiocarbon* 19, no. 3: 355–363. https://doi.org/10.1017/S0033822200003672.

Wang, X. C., T. T. Ge, C. L. Xu, Y. J. Xue, and C. L. Luo. 2016*b*. "Carbon Isotopic (14C and 13C) Characterization of Fossil-Fuel Derived Dissolved Organic Carbon in Wet Precipitation in Shandong Province, China." *Journal of Atmospheric Chemistry* 73: 207–221. https://doi.org/10.1007/s10874-015-9323-3.

Wang, X. C., H. Q. Ma, R. H. Li, Z. S. Song, and J. P. Wu. 2012. "Seasonal Fluxes and Source Variation of Organic Carbon Transported by Two Major Chinese Rivers: The Yellow River and Changjiang (Yangtze) River." *Global Biogeochemical Cycles* 26, no. 2: GB2025. https://doi.org/10.1029/2011GB004130.

Wang, X. C., C. L. Xu, E. M. Druffel, Y. J. Xue, and Y. Z. Qi. 2016*a*. "Two Black Carbon Pools Transported by the Changjiang and Huanghe Rivers in China." *Global Biogeochemical Cycles* 30, no. 12: 1778–1790. https://doi.org/10.1002/2016GB005509.

Wei, B. B., B. Wei, M. Seidel, et al. 2024. "Rapid Down-Slope Transport of Fresh Dissolved Organic Matter to the Deep Ocean in the Eastern North Atlantic." *Geophysical Research Letters* 51, no. 21: e2024GL110349. https://doi.org/10.1029/2024GL110349.

Willey, J. D., R. J. Kieber, M. S. Eyman, and G. B. Avery. 2000. "Rainwater Dissolved Organic Carbon: Concentrations and Global Flux." *Global Biogeochemical Cycles* 14, no. 1: 139–148. https://doi.org/10.1029/1999GB900036.

Williams, P. M., and E. R. M. Druffel. 1987. "Radiocarbon in Dissolved Organic-Matter in the Central North Pacific-Ocean." *Nature* 330: 246–248. https://doi.org/10.1038/330246a0.

Xing, J. W., J. Xing, J. Song, et al. 2019. "Atmospheric Wet Deposition of Dissolved Organic Carbon to a Typical Anthropogenic-Influenced Semi-Enclosed Bay in the Western Yellow Sea, China: Flux, Sources and Potential Ecological Environmental Effects." *Ecotoxicology and Environmental Safety* 182: 109371. https://doi.org/10.1016/j.ecoenv.2019.109371.

Xue, Y. J., L. Zou, T. T. Ge, and X. C. Wang. 2017. "Mobilization and Export of Millennial-Aged Organic Carbon by the Yellow River." *Limnology and Oceanography* 62, no. S1: S95–S111. https://doi.org/10.1002/lno.10579.

Yan, G., and G. Kim. 2012. "Dissolved Organic Carbon in the Precipitation of Seoul, Korea: Implications for Global Wet Depositional Flux of Fossil-Fuel Derived Organic Carbon." *Atmospheric Environment* 59: 117–124. https://doi.org/10.1016/j.atmosenv.2012.05.044.

Yan, G., and G. Kim. 2017. "Speciation and Sources of Brown Carbon in Precipitation at Seoul, Korea: Insights from Excitation-Emission Matrix Spectroscopy and Carbon Isotopic Analysis." *Environmental Science & Technology* 51, no. 20: 11580–11587. https://doi.org/10.1021/acs.est.7b02892.

Yu, M., Z. Guo, X. Wang, et al. 2018. "Sources and Radiocarbon Ages of Aerosol Organic Carbon along the East Coast of China and Implications for Atmospheric Fossil Carbon Contributions to China Marginal Seas." *Science of the Total Environment* 619: 957–965. https://doi.org/10.1016/j.scitotenv.2017.11.201.

Zhou, N., G. L. Zhang, and S. M. Liu. 2022. "Nutrient Exchanges at the Sediment-Water Interface and the Responses to Environmental Changes in the Yellow Sea and East China Sea." *Marine Pollution Bulletin* 176: 113420. https://doi.org/10.1016/j.marpolbul.2022.113420.

Supporting Information

Additional Supporting Information may be found in the online version of this article.

Submitted 22 April 2025
Revised 25 September 2025
Accepted 04 December 2025